

# A Radiative Model for the Weak Scale and Neutrino Mass via Dark Matter

Amine Ahriche,<sup>a,b,1</sup> Kristian L. McDonald<sup>c,2</sup> and Salah Nasri<sup>d,3</sup>

<sup>a</sup> *Department of Physics, University of Jijel, PB 98 Ouled Aissa, DZ-18000 Jijel, Algeria*

<sup>b</sup> *The Abdus Salam International Centre for Theoretical Physics, Strada Costiera 11, I-34014, Trieste, Italy*

<sup>c</sup> *ARC Centre of Excellence for Particle Physics at the Terascale, School of Physics, The University of Sydney, NSW 2006, Australia*

<sup>d</sup> *Physics Department, UAE University, POB 17551, Al Ain, United Arab Emirates*

## Abstract

We present a three-loop model of neutrino mass in which both the weak scale and neutrino mass arise as radiative effects. In this approach, the scales for electroweak symmetry breaking, dark matter, and the exotics responsible for neutrino mass, are related due to an underlying scale-invariance. This motivates the otherwise-independent  $\mathcal{O}(\text{TeV})$  exotic masses usually found in three-loop models of neutrino mass. We demonstrate the existence of viable parameter space and show that the model can be probed at colliders, precision experiments, and dark matter direct-detection experiments.

---

<sup>1</sup>aahriche@ictp.it

<sup>2</sup>klmcd@physics.usyd.edu.au

<sup>3</sup>snasri@uaeu.ac.ae

# 1 Introduction

Radiative symmetry breaking [1] offers an interesting alternative to the conventional Higgs mechanism. In this approach, calculable weakly-coupled radiative effects induce symmetry breaking in classically scale-invariant theories, thereby giving birth to mass — a process known as dimensional transmutation. When applied to the Standard Model (SM), it is well known that radiative symmetry breaking is not viable, due to the destabilizing influence of the heavy top quark. However, the SM is known to be incomplete, due to e.g. an absence of massive neutrinos and the need to incorporate dark matter (DM). It is therefore interesting to consider the viability of radiative symmetry breaking within SM extensions.

The addition of massive neutrinos and DM to the SM likely requires new degrees of freedom. When considering radiative symmetry breaking, there are a number of relevant considerations that can guide the choice of beyond-SM fields. The destabilizing radiative corrections from the top quark can be overcome by bosonic degrees of freedom with mass  $\gtrsim 200$  GeV. In principle these states could be much heavier than the TeV scale. However, radiative symmetry breaking typically introduces a single scale into a theory, with other mass and symmetry breaking scales related to this scale.<sup>4</sup> Consequently both the electroweak scale and the mass scale for exotics may be related via dimensionless parameters. Thus, absent hierarchically small parameters [2], one anticipates exotics with  $\mathcal{O}(\text{TeV})$  masses.

In the LHC era, TeV scale exotics are of particular interest. However, efforts to generate tiny neutrino masses via weak-scale exotics can struggle to achieve the necessary mass-suppression, relative to the weak scale, without invoking tiny couplings. Perhaps the most obvious exception are models with radiative neutrino mass, as the inherent loop-suppression in such models can motivate lighter new physics. From this perspective, three-loop models of neutrino mass are particularly compelling, as the new physics is expected to be  $\mathcal{O}(\text{TeV})$ .

These considerations focus our attention on scale-invariant models with three-loop neutrino mass. If we also seek to address the DM problem, a minimal approach would see the DM play a role in either generating neutrino mass or triggering electroweak symmetry breaking. Thus, we arrive at a picture in which *both the weak scale and neutrino mass arise as radiative effects, with the weak scale, the DM mass, and the mass scale for the exotics that induce neutrino mass, all finding a common birth, via dimensional transmutation.* This picture can address short-comings of the SM, while also explaining why the exotics required in three-loop neutrino mass models have (otherwise independent) masses of  $\mathcal{O}(\text{TeV})$  — a common ancestry requires that they be related to the weak scale.

In this work we present a scale-invariant model for three-loop neutrino mass that contains a fermionic DM candidate. We explore the model in detail and present feasible parameter space that achieves the correct DM relic abundance, while generating viable symmetry breaking and neutrino masses — all compatible with low-energy constraints. As per usual for scale-invariant frameworks, the model predicts a dilaton. However, here the dilaton has the dual role of allowing electroweak symmetry breaking and simultaneously sourcing the lepton number violation that allows radiative neutrino masses. We note that a number of earlier works studied relationships between the origin of neutrino mass and DM, see e.g. Refs. [3, 4, 5, 6, 7, 8]. There has also been much interest in scale-invariant models in recent years, see e.g. Refs. [9, 10, 11, 12, 13, 14].

The structure of this paper is as follows. In Section 2 we introduce the model and detail the symmetry breaking sector. We turn our attention to the origin of neutrino mass in Section 3

---

<sup>4</sup>The exceptions being when a theory also contains a confining gauge sector, as with QCD in the SM, or a completely decoupled hidden sector possessing its own symmetry breaking and/or confining pattern.

and discuss various constraints in Section 4. Dark matter is discussed in Section 5 and our main analysis and results appear in Section 6. Conclusions are drawn in Section 7.

## 2 A Scale-Invariant Three-Loop Model

We consider a classically scale-invariant (SI) extension of the SM in which neutrino mass appears at the three-loop level. The SM is extended by the addition of two charged scalars,  $S_{1,2}^+ \sim (1, 1, 2)$ , three singlet fermions,  $N_{iR} \sim (1, 1, 0)$ , with  $i \in \{1, 2, 3\}$  labeling generations, and a singlet scalar,  $\phi \sim (1, 1, 0)$ .<sup>5</sup> A  $Z_2$  symmetry with action  $\{S_2, N_R\} \rightarrow \{-S_2, -N_R\}$  is imposed, with all other fields being  $Z_2$ -even. This symmetry remains exact in the full theory, making the lightest  $Z_2$ -odd field a stable DM candidate, which should be taken as the lightest fermion,  $N_1 \equiv N_{\text{DM}}$ , to avoid a cosmologically-excluded stable charged particle. The scalar  $\phi$  plays a key role in triggering electroweak symmetry breaking, as explained below, and also ensures that lepton number symmetry is explicitly broken, thereby allowing radiative neutrino mass.

Consistent with the SI and  $Z_2$  symmetries, the Lagrangian contains the following terms:

$$\mathcal{L} \supset - \{f_{\alpha\beta} \bar{L}_\alpha^c L_\beta S_1^+ + g_{i\alpha} \bar{N}_i^c S_2^+ e_{\alpha R} + \text{H.c.}\} - \frac{1}{2} \tilde{y}_i \phi \bar{N}_i^c N_i - V(H, S_{1,2}, \phi), \quad (1)$$

where Greek letters label SM flavors,  $\alpha, \beta \in \{e, \mu, \tau\}$ , and  $f_{\alpha\beta}$ ,  $g_{i\alpha}$  and  $\tilde{y}_i$  are Yukawa couplings. The  $Z_2$  symmetry forbids the term  $\bar{L} \tilde{H} N_R$ , which would otherwise generate tree-level neutrino masses after the SM scalar  $H \sim (1, 2, 1)$  develops a VEV. The potential  $V(H, S_{1,2}, \phi)$  is the most-general potential consistent with the SI and  $Z_2$  symmetries.

### 2.1 Symmetry Breaking

We are interested in parameter space where both  $\phi$  and  $H$  acquire nonzero vacuum expectation values (VEVs),  $\langle H \rangle \neq 0$  and  $\langle \phi \rangle \neq 0$ . This breaks both the SI and electroweak symmetries while preserving the  $Z_2$  symmetry. The most-general scalar potential includes the terms

$$V_0(H, S_{1,2}, \phi) \supset \lambda_H |H|^4 + \frac{\lambda_{\phi H}}{2} |H|^2 \phi^2 + \frac{\lambda_\phi}{4} \phi^4 + \frac{\lambda_S}{4} (S_1^-)^2 (S_2^+)^2 + \sum_{a=1,2} \frac{1}{2} (\lambda_{Ha} |H|^2 + \lambda_{\phi a} \phi^2) |S_a|^2. \quad (2)$$

The physical spectrum contains two charged scalars  $S_{1,2}^+$ , and two neutral scalars, denoted as  $h_{1,2}$ . A complete analysis of the potential requires the inclusion of the leading-order radiative corrections. However, in general the full one-loop corrected potential is not analytically tractable. None the less, simple analytic expressions can be obtained if one neglects the loop corrections involving only the scalars  $h_{1,2}$ . This approximation is justified, as one of the scalars is massless at tree-level (the dilaton,  $h_2$ ) while the SM-like Higgs has mass  $M_{h_1} \approx 125$  GeV. The corresponding radiative corrections are dominated by the top quark and the beyond-SM scalars  $S_{1,2}^+$ , which must be heavier than the top quark in order to allow viable symmetry breaking and evade experimental constraints.

---

<sup>5</sup>Quantities in parentheses refer to quantum numbers under the SM gauge symmetry  $SU(3)_c \otimes SU(2)_L \otimes U(1)_Y$ .

Adopting this approximation, the one-loop corrected potential for the CP-even neutral scalars is

$$V_{1-l}(h, \phi) = \frac{\lambda_H}{4} h^4 + \frac{\lambda_{\phi H}}{4} \phi^2 h^2 + \frac{\lambda_\phi}{4} \phi^4 + \sum_{i=\text{all fields}} n_i G(m_i^2(h, \phi)), \quad (3)$$

$$G(\eta) = \frac{\eta^2}{64\pi^2} \left[ \log \frac{\eta}{\Lambda^2} - \frac{3}{2} \right], \quad (4)$$

where  $\Lambda$  is the renormalization scale,  $n_i$  are the field multiplicities, and we employ the unitary gauge, with  $H = (0, h/\sqrt{2})^T$ . The sum is over all fields, neglecting the light SM fermions (all but the top quark) and the (to be determined) neutral scalar mass-eigenstates  $h_{1,2}$ . Due to the SI symmetry, the field-dependent masses can be written as

$$m_i^2(h, \phi) = \frac{\alpha_i}{2} h^2 + \frac{\beta_i}{2} \phi^2, \quad (5)$$

for constant  $\alpha_i$  and  $\beta_i$ .

Dimensional transmutation introduces a dimensionful parameter into the theory in exchange for one of the dimensionless couplings. In the present model, an analysis of the potential shows that a minimum with  $\langle h \rangle \equiv v \neq 0$  and  $\langle \phi \rangle \equiv x \neq 0$  exists for  $\lambda_{\phi H} < 0$ , and is triggered at the scale where the couplings satisfy the relation

$$2 \left\{ \lambda_H \lambda_\phi + \frac{\lambda_H}{x^2} \sum_i n_i \left\{ \beta_i - \alpha_i \frac{v^2}{x^2} \right\} G'(m_i^2) \right\}^{1/2} + \lambda_{\phi H} + \frac{2}{x^2} \sum_i n_i \alpha_i G'(m_i^2) = 0, \quad (6)$$

with  $G'(\eta) = \partial G(\eta) / \partial \eta$ . The further condition

$$-\frac{\lambda_{\phi H}}{2\lambda_H} = \frac{v^2}{x^2} + \sum_i \frac{n_i \alpha_i}{\lambda_H x^2} G'(m_i^2), \quad (7)$$

is also satisfied at the minimum. Thus, for  $\lambda_{\phi H, H} = \mathcal{O}(1)$  one has  $v \sim x$  and the exotic scale is naively expected around the TeV scale. Note that Eqs. (6) and (7) ensure that the tadpoles vanish.<sup>6</sup>

Defining the one-loop quartic couplings as

$$\lambda_\phi^{1-l} = \frac{1}{6} \frac{\partial^4 V_{1-l}}{\partial \phi^4}, \quad \lambda_H^{1-l} = \frac{1}{6} \frac{\partial^4 V_{1-l}}{\partial h^4}, \quad \lambda_{\phi H}^{1-l} = \frac{\partial^4 V_{1-l}}{\partial h^2 \partial \phi^2}, \quad (8)$$

vacuum stability at one-loop requires that the following conditions be satisfied:

$$\lambda_H^{1-l}, \lambda_\phi^{1-l}, \lambda_{\phi H}^{1-l} + 2\sqrt{\lambda_H^{1-l} \lambda_\phi^{1-l}} > 0. \quad (9)$$

We must also impose the condition  $\lambda_{\phi H}^{1-l} < 0$  to ensure that the vacuum with  $v \neq 0$  and  $x \neq 0$  is the ground state.<sup>7</sup> Eq. (9) also guarantees that the eigenmasses-squared for the CP-even neutral scalars are strictly positive, and forces one of the beyond-SM scalars  $S_{1,2}^+$  be the heaviest particle in the spectrum.

---

<sup>6</sup>To our level of approximation, Eqs. (6) and (7) are the loop-corrected generalizations of the standard tree-level results,  $4\sqrt{\lambda_H(\Lambda) \lambda_\phi(\Lambda)} + \lambda_{\phi H}(\Lambda) = 0$  and  $\lambda_{\phi H}/2\lambda_H = v^2/x^2$  [15].

<sup>7</sup>For  $\lambda_{\phi H}^{1-l} > 0$  the vacuum with only one nonzero VEV is preferred.

## 2.2 The Scalar Spectrum

The mass matrix for the neutral scalars is denoted as

$$V_{1-l}(h, \phi) \supset \frac{1}{2}(h, \phi) \begin{pmatrix} m_{hh}^2 & m_{h\phi}^2 \\ m_{h\phi}^2 & m_{\phi\phi}^2 \end{pmatrix} \begin{pmatrix} h \\ \phi \end{pmatrix}, \quad (10)$$

where the mass parameters  $m_{hh}$ ,  $m_{\phi\phi}$  and  $m_{h\phi}$  are calculated from the loop-corrected potential  $V_{1-l}(h, \phi)$ . The mass eigenstates are labeled as

$$h_1 = \cos \theta_h h - \sin \theta_h \phi, \quad h_2 = \sin \theta_h h + \cos \theta_h \phi, \quad (11)$$

with the eigenvalues and mixing angles given by

$$\begin{aligned} M_{h_{1,2}}^2 &= \frac{1}{2} \left\{ m_{11}^2 + m_{22}^2 \pm \sqrt{(m_{22}^2 - m_{11}^2)^2 + 4m_{12}^4} \right\}, \\ \tan 2\theta_h &= \frac{2m_{12}^2}{m_{22}^2 - m_{11}^2}. \end{aligned} \quad (12)$$

Here  $h_1$  is a massive SM-like scalar and  $h_2$  is a pseudo-Goldstone boson associated with SI symmetry breaking — the latter is massless at tree-level but acquires mass at the loop-level. The tree-level expression for the SM-like scalar mass is

$$M_{h_1}^2 = (2\lambda_H - \lambda_{\phi H})v^2 \simeq 125 \text{ GeV}, \quad (13)$$

and the tree-level expression for the mixing angle is

$$c_h \equiv \cos \theta_h = \frac{x}{\sqrt{x^2 + v^2}}, \quad s_h \equiv \sin \theta_h = \frac{v}{\sqrt{x^2 + v^2}}. \quad (14)$$

Due to the SI symmetry, the parameters in the model are somewhat constrained, with  $\lambda_\phi$  and  $\lambda_{\phi H}$  fixed by Eqs. (6) and (7) while the Higgs mass  $M_{h_1} \simeq 125 \text{ GeV}$  fixes  $\lambda_H$ .

The tree-level masses for the charged scalars,  $S_{1,2}^+$ , are

$$M_{S_a}^2 = \frac{1}{2} \left\{ \lambda_{\phi a} x^2 + \lambda_{Ha} \frac{v^2}{2} \right\} \quad \text{for } a = 1, 2, \quad (15)$$

where  $S_1^+$  and  $S_2^+$  do not mix due to the  $Z_2$  symmetry. In our numerical analysis below we employ the full loop-corrected expressions for the scalar masses and mixing, as is necessary to obtain  $M_{h_2} \neq 0$ . Note that a useful approximation for  $M_{h_2}$  is [16]

$$M_{h_2}^2 \simeq \frac{1}{8\pi^2(\langle\phi\rangle^2 + \langle h\rangle^2)} \left\{ M_{h_1}^4 + 6M_W^4 + 3M_Z^4 - 12M_t^4 + 2 \sum_{a=1}^2 M_{S_a}^4 - 2 \sum_{i=1}^3 M_{N_i}^4 \right\}, \quad (16)$$

which shows that one of the beyond-SM scalars  $S_{1,2}$  must be the heaviest beyond-SM state in order to ensure  $M_{h_2} > 0$ .

As mentioned already, we expect the VEVs to be of a similar scale,  $\langle\phi\rangle \sim \langle h\rangle$ , as evidenced by Eq. (7). For completeness, however, we note that there is a technically natural limit in which one obtains  $\langle\phi\rangle \gg \langle h\rangle$ . This arises when *all* the couplings to  $\phi$  are taken to be hierarchically small, namely  $\{\tilde{y}_i, \lambda_{\phi H}, \lambda_{\phi 1,2}\} \ll 1$ , with the masses  $M_{h_1}$ ,  $M_N$  and  $M_{S_{1,2}}$  held at  $\mathcal{O}(\text{TeV})$ . This feature reflects the fact that  $\phi$  decouples in the limit  $\{\tilde{y}_i, \lambda_{\phi H}, \lambda_{\phi 1,2}\} \rightarrow 0$ , up to gravitational effects [17]. In this limit we expect the model to be very similar to the KNT model [3], but with a light, very weakly-coupled scalar in the spectrum,  $h_2$ . Absent a compelling motivation for such hierarchically small parameters, we restrict our attention to values of  $\langle\phi\rangle \leq 5 \text{ TeV}$ .

### 3 Neutrino Mass

We now turn to the origin of neutrino mass. The  $Z_2$ -odd fermions,  $N_i$ , develop masses  $M_{N_i} = \tilde{y}_i \langle \phi \rangle$ , and do not mix with SM leptons due to the  $Z_2$  symmetry. We order their masses as  $M_{\text{DM}} \equiv M_{N_1} < M_{N_2} < M_{N_3}$ . SM neutrinos, on the other hand, acquire mass radiatively. The combination of the Yukawa interactions in Eq. (1) and the term

$$V(H, S_{1,2}, \phi) \supset \frac{\lambda_s}{4} (S_1^-)^2 (S_2^+)^2, \quad (17)$$

in the scalar potential, explicitly break lepton number symmetry. Consequently neutrino masses appear at the three-loop level as shown in Figure 1.

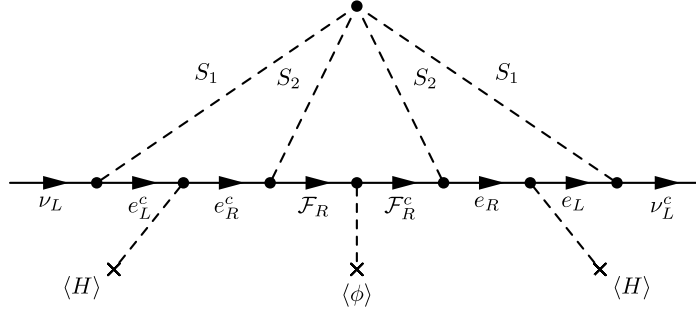


Figure 1: Three-loop diagram for neutrino mass in a scale-invariant model.

Calculating the loop diagram, the mass matrix has the form

$$(\mathcal{M}_\nu)_{\alpha\beta} = \frac{\lambda_s}{(4\pi^2)^3} \frac{m_\sigma m_\rho}{M_{S_2}} g_{\sigma i}^* g_{\rho i}^* f_{\alpha\sigma} f_{\beta\rho} \times F_{loop} \left( \frac{M_{N_i}^2}{M_{S_2}^2}, \frac{M_{S_1}^2}{M_{S_2}^2} \right), \quad (18)$$

where  $m_{\sigma,\rho}$  denote charged lepton masses and the function  $F_{loop}(x, y)$  encodes the loop integrals [5]

$$F_{loop}(\alpha, \beta) = \frac{\sqrt{\alpha}}{8\beta^2} \int_0^\infty dr \frac{r}{r + \alpha} \left( \int_0^1 dx \ln \frac{x(1-x)r + (1-x)\beta + x}{x(1-x)r + x} \right)^2. \quad (19)$$

One can relate the neutrino mass matrix to the elements of the Pontecorvo-Maki-Nakawaga-Sakata (PMNS) mixing matrix [18] elements, we parameterize the latter as

$$U_\nu = \begin{pmatrix} c_{12}c_{13} & c_{13}s_{12} & s_{13}e^{-i\delta_d} \\ -c_{23}s_{12} - c_{12}s_{13}s_{23}e^{i\delta_d} & c_{12}c_{23} - s_{12}s_{13}s_{23}e^{i\delta_d} & c_{13}s_{23} \\ s_{12}s_{23} - c_{12}c_{23}s_{13}e^{i\delta_d} & -c_{12}s_{23} - c_{23}s_{12}s_{13}e^{i\delta_d} & c_{13}c_{23} \end{pmatrix} \times U_m, \quad (20)$$

with  $\delta_d$  the Dirac phase and  $U_m = \text{diag}(1, e^{i\theta_\alpha/2}, e^{i\theta_\beta/2})$  encoding the Majorana phase dependence. The shorthand  $s_{ij} \equiv \sin \theta_{ij}$  and  $c_{ij} \equiv \cos \theta_{ij}$  refers to the mixing angles. For our numerical scans (discussed below) we fit to the best-fit experimental values for the mixing angles and mass-squared differences:  $s_{12}^2 = 0.320_{-0.017}^{+0.016}$ ,  $s_{23}^2 = 0.43_{-0.03}^{+0.03}$ ,  $s_{13}^2 = 0.025_{-0.003}^{+0.003}$ ,  $|\Delta m_{13}^2| = 2.55_{-0.09}^{+0.06} \times 10^{-3} \text{eV}^2$  and  $\Delta m_{21}^2 = 7.62_{-0.19}^{+0.19} \times 10^{-5} \text{eV}^2$  [19]. Furthermore, we require that the contribution to neutrino-less double beta decay in this model satisfies the current bound. Within these ranges, one determines the parameter space where viable neutrino masses and mixing occur in the model.

## 4 Experimental Constraints

In this section we discuss the constraints on the model from the lepton flavor violating process  $\mu \rightarrow e\gamma$ , the electroweak precision tests, the invisible Higgs decay, and the effect on  $h\gamma\gamma$  process.

### 4.1 Lepton flavor

Flavor changing processes like  $\mu \rightarrow e + \gamma$  arise via loop diagrams containing virtual charged scalars and give important constraints on the model. At one-loop the branching ratio for  $\mu \rightarrow e + \gamma$  is

$$\begin{aligned} \mathcal{B}(\mu \rightarrow e\gamma) &= \frac{\Gamma(\mu \rightarrow e + \gamma)}{\Gamma(\mu \rightarrow e + \nu + \bar{\nu})} \\ &\simeq \frac{\alpha v^4}{384\pi} \times \left\{ \frac{|f_{\mu\tau} f_{\tau e}^*|^2}{M_{S_1}^4} + \frac{36}{M_{S_2}^4} \left| \sum_i g_{ie}^* g_{i\mu} F_2(M_i^2/M_{S_2}^2) \right|^2 \right\}, \end{aligned} \quad (21)$$

where  $F_2(R) = [1 - 6R + 3R^2 + 2R^3 - 6R^2 \log R]/[6(1 - R)^4]$ . The corresponding expression for  $\mathcal{B}(\tau \rightarrow \mu + \gamma)$  follows from a simple change of flavor labels in Eq. (21). Similarly, the one-loop contributions to the anomalous magnetic moment of the muon are

$$\delta a_\mu = -\frac{m_\mu^2}{16\pi^2} \left\{ \sum_{\alpha \neq \mu} \frac{|f_{\mu\alpha}|^2}{6M_{S_1}^2} + \sum_i \frac{|g_{i\mu}|^2}{M_{S_2}^2} F_2(M_i^2/M_{S_2}^2) \right\}. \quad (22)$$

Null-results from searches for neutrino-less double-beta decay give an additional constraint of  $(\mathcal{M}_\nu)_{ee} \lesssim 0.35$  eV [20], though we find this is easily satisfied.

### 4.2 Electroweak precision tests

In principle, precision electroweak measurements can provide additional constraints. The oblique parameters characterizing new physics effects are given by [21]

$$\frac{\alpha}{4s_W^2 c_W^2} S = \frac{A_{ZZ}(M_Z^2) - A_{ZZ}(0)}{M_Z^2} - \frac{\partial A_{\gamma\gamma}(q^2)}{\partial q^2} \Big|_{q^2=0} + \frac{c_W^2 - s_W^2}{c_W s_W} \frac{\partial A_{\gamma Z}(q^2)}{\partial q^2} \Big|_{q^2=0}, \quad (23)$$

$$\alpha T = \frac{A_{WW}(0)}{M_W^2} - \frac{A_{ZZ}(0)}{M_Z^2}. \quad (24)$$

Here,  $\alpha = e^2/(4\pi) = g^2 s_w^2/(4\pi)$  is the fine-structure constant,  $s_w = \sin \theta_w$  and  $c_w = \cos \theta_w$  are the sine and cosine, respectively, of the Weinberg angle  $\theta_w$ , and the functions  $A_{VV'}(q^2)$  are the coefficients of  $g^{\mu\nu}$  in the vacuum-polarization tensors  $\Pi_{VV'}^{\mu\nu}(q) = g^{\mu\nu} A_{VV'}(q^2) + q^\mu q^\nu B_{VV'}(q^2)$ , where  $VV'$  could be either  $\gamma\gamma$ ,  $\gamma Z$ ,  $ZZ$ , or  $WW$ . In our model, the oblique parameters are given by [22]

$$\begin{aligned} \Delta T &= \frac{3}{16\pi s_w^2 M_W^2} \left\{ c_h^2 [F(M_Z^2, M_{h_1}^2) - F(M_W^2, M_{h_1}^2)] + s_h^2 [F(M_Z^2, M_{h_2}^2) - F(M_W^2, M_{h_2}^2)] \right. \\ &\quad \left. - [F(M_Z^2, M_h^2) - F(M_W^2, M_h^2)] \right\}, \end{aligned} \quad (25)$$



$$\Delta S = \frac{1}{24\pi} \left\{ 4s_w^4 G(M_{S_1}^2, M_{S_1}^2, M_Z^2) + 4s_w^4 G(M_{S_2}^2, M_{S_2}^2, M_Z^2) + c_h^2 \ln \frac{M_{h_1}^2}{M_h^2} + s_h^2 \ln \frac{M_{h_2}^2}{M_h^2} + c_h^2 \hat{G}(M_{h_1}^2, M_Z^2) + s_h^2 \hat{G}(M_{h_2}^2, M_Z^2) - \hat{G}(M_h^2, M_Z^2) \right\}, \quad (26)$$

where the functions  $F$ ,  $G$  and  $\hat{G}$  are given in the appendix and  $M_h = 125.09$  GeV denotes the reference value.

### 4.3 Higgs invisible decay

The model can also face constraints from the invisible Higgs decay,  $\mathcal{B}(h \rightarrow inv) < 17\%$  [23]. In our case we have  $inv \equiv \{h_2 h_2\}, \{N_{DM} N_{DM}\}$ , when kinematically available. The corresponding decay widths are given by

$$\begin{aligned} \Gamma(h_1 \rightarrow h_2 h_2) &= \frac{1}{32\pi} \frac{(\lambda_{122})^2}{M_{h_1}} \left(1 - \frac{4M_{h_2}^2}{M_{h_1}^2}\right)^{\frac{1}{2}} \Theta(M_{h_1} - 2M_{h_2}), \\ \Gamma(h_1 \rightarrow N_{DM} N_{DM}) &= \frac{\tilde{y}_{DM}^2 s_h^2}{16\pi} M_{h_1} \left(1 - \frac{4M_{DM}^2}{M_{h_1}^2}\right)^{\frac{3}{2}} \Theta(M_{h_1} - 2M_{DM}). \end{aligned} \quad (27)$$

The effective cubic coupling  $\lambda_{122}$  is defined below in Eq. (35). However, due to the SI symmetry, we find that  $\lambda_{122}$  vanishes at tree-level so the decay to  $h_2$  pairs is highly suppressed.<sup>8</sup>

### 4.4 The Higgs decay channel $h \rightarrow \gamma\gamma$

The existence of extra charged scalars modifies the two Higgs branching ratios  $\mathcal{B}(h \rightarrow \gamma\gamma, \gamma Z)$ , and this deviation can be parameterized by the ratios:

$$R_{\gamma\gamma} = \frac{\mathcal{B}(h \rightarrow \gamma\gamma)}{\mathcal{B}^{SM}(h \rightarrow \gamma\gamma)} = \left| 1 + \frac{v}{2c_h} \frac{\frac{\vartheta_1}{m_{S_1}^2} A_0^{\gamma\gamma}(\tau_{S_1}) + \frac{\vartheta_2}{m_{S_2}^2} A_0^{\gamma\gamma}(\tau_{S_2})}{A_1^{\gamma\gamma}(\tau_W) + N_c Q_t^2 A_{1/2}^{\gamma\gamma}(\tau_t)} \right|^2, \quad (28)$$

$$R_{\gamma Z} = \frac{\mathcal{B}(h \rightarrow \gamma Z)}{\mathcal{B}^{SM}(h \rightarrow \gamma Z)} = \left| 1 + \frac{s_w v}{c_h} \frac{\frac{\vartheta_1}{m_{S_1}^2} A_0^{\gamma Z}(\tau_{S_1}, \lambda_{S_1}) + \frac{\vartheta_2}{m_{S_2}^2} A_0^{\gamma Z}(\tau_{S_2}, \lambda_{S_2})}{c_w A_1^{\gamma Z}(\tau_W, \lambda_W) + \frac{2(1-8s_w^2/3)}{c_w} A_{1/2}^{\gamma Z}(\tau_t, \lambda_t)} \right|^2, \quad (29)$$

where  $\tau_X = M_{h_1}^2/4M_X^2$  and  $\lambda_X = M_Z^2/4M_X^2$ , with  $M_X$  is the mass of the charged particle  $X$  running in the loop,  $N_c = 3$  is the color number,  $Q_t$  is the electric charge of the top quark in unit of  $|e|$ , and the loop amplitudes  $A_i$  for spin 0, spin 1/2 and spin 1 particle contribution [24], which are given in the appendix. Here  $\vartheta_i$ , are the SM-like Higgs couplings to the pairs of charged scalars  $S_{1,2}^\pm$ , which are given by

$$\vartheta_a = c_h \lambda_{Ha} v + s_h \lambda_{\phi a} x. \quad (30)$$

The effect of the charged scalars on (28) and (29) depends on the masses for  $S_a^\pm$ , the sign and the strength of their couplings to the SM Higgs doublet and the neutral singlet and on the mixing angle  $\theta_h$ . One can use the reported results from LHC to constraints these parameters.

---

<sup>8</sup>Note that  $h_2$  decays to SM states, much like a light SM Higgs boson but with suppression from the mixing angle,  $s_h^2$ . However, currently there are no dedicated ATLAS or CMS searches for light scalars in the channels  $2b$ ,  $2\tau$  or  $2\gamma$ , so we classify the decay  $h_1 \rightarrow h_2 h_2$  as invisible. In practise the suppression of  $\Gamma(h_1 \rightarrow h_2 h_2)$  due to SI symmetry renders this point moot.



## 5 Dark Matter

### 5.1 Annihilation Cross Sections

The lightest  $Z_2$ -odd field is a stable DM candidate. As mentioned already, the lightest exotic fermion  $N_{\text{DM}} \equiv N_1$  is the only viable DM candidate in the model. The relic density is given by [25]

$$\Omega_{\text{DM}} h^2 = \frac{1.04 \times 10^9 \text{GeV}^{-1}}{M_{\text{Pl}}} \frac{1}{\sqrt{g_*(T_f)} \int_{x_f}^{\infty} \langle \sigma v \rangle (x) x^{-2} dx}, \quad (31)$$

where  $M_{\text{Pl}} = 1.22 \times 10^{19} \text{ GeV}$  is the Planck scale,  $g_*(T)$  is the total effective number of relativistic particle at temperature  $T$ , and  $x_f = M_{\text{DM}}/T_f$  represents the freeze-out temperature, which can be computed from

$$x_f = \ln \frac{0.03 M_{\text{Pl}} M_{\text{DM}} \langle \sigma v_r(x_f) \rangle}{\sqrt{T_f} x_f}, \quad (32)$$

with  $\langle \sigma v_r \rangle$  is the thermally averaged annihilation cross-section of  $N_1$  into all kinematically accessible final state particles. As will be discussed in the next section, we require that  $\Omega_{N_1} h^2$  to be in agreement with the observed value of the dark matter relic density [26].

The field  $N_1$  couples to SM leptons through the Yukawa couplings  $g_{1\alpha}$ , and can annihilate into charged lepton pairs. Neglecting final-state lepton masses, the corresponding cross section is

$$\sum_{\alpha, \beta} \sigma(N_{\text{DM}} N_{\text{DM}} \rightarrow \ell_{\alpha} \ell_{\beta}) \simeq \sum_{\alpha, \beta} \frac{|g_{1\alpha} g_{1\beta}^*|^2}{48\pi} \frac{M_{\text{DM}}^2 (M_{S_2}^4 + M_{\text{DM}}^4)}{(M_{S_2}^2 + M_{\text{DM}}^2)^4} v_r. \quad (33)$$

Here  $v_r$  is the relative velocity of the initial-state particles in the centre-of-mass (CoM) frame and we retained only the leading ( $p$ -wave) term in the small  $v_r$  expansion.<sup>9</sup>

The DM field also couples to the scalars  $h_{1,2}$ , via the interaction  $-\frac{1}{2} \tilde{y}_{\text{DM}} \phi \overline{N_{\text{DM}}^c} N_{\text{DM}}$  in the Yukawa Lagrangian. This allows three distinct types of annihilations into scalar pairs, namely  $N_{\text{DM}} N_{\text{DM}} \rightarrow h_1 h_2$ , and  $N_{\text{DM}} N_{\text{DM}} \rightarrow h_a h_a$  with  $a = 1, 2$ . To calculate the cross sections we write the relevant Lagrangian terms as follows:

$$\mathcal{L} \supset -\frac{1}{2} \sum_a y_a h_a \overline{N_{\text{DM}}^c} N_{\text{DM}} - \frac{1}{2} \sum_{a, b, a \neq b} \lambda_{aab} h_a^2 h_b - \frac{1}{6} \sum_a \lambda_{aaa} h_a^3, \quad (34)$$

with the Yukawa couplings defined as  $y_1 = s_h \tilde{y}_{\text{DM}}$  and  $y_2 = c_h \tilde{y}_{\text{DM}}$ . At tree-level the effective cubic scalar couplings are given by

$$\begin{aligned} \lambda_{111} &= 6\lambda_{\text{H}} c_h^3 v - 3\lambda_{\phi\text{H}} c_h^2 s_h v + 3\lambda_{\phi\text{H}} c_h s_h^2 v - 6\lambda_{\phi} s_h^3 x, \\ \lambda_{112} &= \lambda_{\phi\text{H}} c_h^3 x + 2c_h^2 s_h (3\lambda_{\text{H}} - \lambda_{\phi\text{H}}) v + 2c_h s_h^2 (3\lambda_{\phi} - \lambda_{\phi\text{H}}) x + \lambda_{\phi\text{H}} s_h^3 v, \\ \lambda_{222} &= \lambda_{122} = 0, \end{aligned} \quad (35)$$

while we use the full one-loop results that can be derived from the loop-corrected potential following [27]. The absence of cubic interactions  $h_1 h_2^2$  and  $h_2^3$ , at leading order, is a general feature of SI models.

---

<sup>9</sup>For finite lepton masses the  $s$ -wave contribution is suppressed by the small factor  $m_{\alpha} m_{\beta} / M_{S_2}^2$ .

Taking the small relative-velocity limit in the CoM frame, the cross section for annihilations into identical scalars is

$$\begin{aligned} & \sigma(N_{\text{DM}}N_{\text{DM}} \rightarrow h_a h_a) \\ = & \frac{v_r}{192\pi} \left\{ \frac{3y_a^2 \lambda_{aaa}^2}{(4M_{\text{DM}}^2 - M_a^2)^2} + \frac{6y_a y_b \lambda_{aaa} \lambda_{aab}}{(4M_{\text{DM}}^2 - M_a^2)(4M_{\text{DM}}^2 - M_b^2)} + \frac{3y_b^2 \lambda_{aab}^2}{(4M_{\text{DM}}^2 - M_b^2)^2} - \frac{8y_a^3 \lambda_{aaa} M_{\text{DM}}(5M_{\text{DM}}^2 - 2M_a^2)}{(4M_{\text{DM}}^2 - M_a^2)(2M_{\text{DM}}^2 - M_a^2)^2} \right. \\ & \left. - \frac{8y_a^2 y_b \lambda_{aab} M_{\text{DM}}(5M_{\text{DM}}^2 - 2M_a^2)}{(4M_{\text{DM}}^2 - M_b^2)(2M_{\text{DM}}^2 - M_a^2)^2} + \frac{16y_a^4 M_{\text{DM}}^2(9M_{\text{DM}}^4 - 8M_{\text{DM}}^2 M_a^2 + 2M_a^4)}{(2M_{\text{DM}}^2 - M_a^2)^4} \right\}, \end{aligned} \quad (36)$$

where  $a, b = 1, 2$ , with  $a \neq b$ , and we denote the scalar masses as  $M_a \equiv M_{h_a}$ . Note that annihilations into  $h_2$ -pairs only proceed via the  $t/u$ -channels while there are  $s$ -channel contributions for final states with  $h_1$ -pairs. The general result for annihilations into distinct scalars is:

$$\begin{aligned} & \sigma(N_{\text{DM}}N_{\text{DM}} \rightarrow h_1 h_2) \\ = & \frac{v_r}{192\pi} \left\{ 3 \times \left[ \sum_{a,b,a \neq b} \frac{y_a \lambda_{aab}}{(4M_{\text{DM}}^2 - M_a^2)} \right]^2 + \frac{y_1^2 y_2^2}{M_{\text{DM}}^2 (4M_{\text{DM}}^2 - M_1^2 - M_2^2)^4} \times \mathcal{N}(M_{\text{DM}}, M_1, M_2) \right. \\ & \left. - \frac{2y_1 y_2}{M_{\text{DM}}} \frac{(80M_{\text{DM}}^4 - (M_1^2 - M_2)^2 - 16M_{\text{DM}}^2(M_1^2 + M_2^2))}{(4M_{\text{DM}}^2 - M_1^2 - M_2^2)^2} \left[ \sum_{a,b,a \neq b} \frac{y_a \lambda_{aab}}{(4M_{\text{DM}}^2 - M_a^2)} \right] \right\}, \end{aligned} \quad (37)$$

where we defined the function  $\mathcal{N}(M_{\text{DM}}, M_1, M_2)$  by:

$$\begin{aligned} \mathcal{N}(M_{\text{DM}}, M_1, M_2) = & 2304M_{\text{DM}}^8 + (M_1^2 - M_2^2)^4 - 1024M_{\text{DM}}^6(M_1^2 + M_2^2) \\ & + 32M_{\text{DM}}^4(3M_1^4 + 10M_1^2 M_2^2 + 3M_2^4). \end{aligned}$$

In the parameter space with very small mixing,  $s_h \ll 1$ , the total cross section for annihilation into scalars simplifies:

$$\sigma_s \equiv \sum_a \sigma(N_{\text{DM}}N_{\text{DM}} \rightarrow h_a h_a) + \sigma(N_{\text{DM}}N_{\text{DM}} \rightarrow h_1 h_2) \simeq \sigma(N_{\text{DM}}N_{\text{DM}} \rightarrow h_2 h_2), \quad (38)$$

with

$$\begin{aligned} \sigma(N_{\text{DM}}N_{\text{DM}} \rightarrow h_2 h_2) & \simeq \frac{y_2^4 v_r}{12\pi} \frac{\{9M_{\text{DM}}^6 - 8M_2^2 M_{\text{DM}}^4 + 2M_2^4 M_{\text{DM}}^2\}}{(2M_{\text{DM}}^2 - M_2^2)^4} \\ & \simeq \frac{3y_2^4 v_r}{64\pi} \frac{1}{M_{\text{DM}}^2}, \end{aligned} \quad (39)$$

where the further limit of  $M_{\text{DM}} \gg M_{h_2}$  is taken in the last line.

## 5.2 Direct Detection

Concerning direct-detection experiments, the effective low-energy Lagrangian responsible for interactions between the DM and quarks is given by

$$\mathcal{L}_{N_1-q}^{(eff)} = a_q \bar{q} q N_{\text{DM}}^c N_{\text{DM}}, \quad (40)$$

with

$$a_q = -\frac{s_h c_h M_q M_{\text{DM}}}{2v x} \left[ \frac{1}{M_{h_1}^2} - \frac{1}{M_{h_2}^2} \right]. \quad (41)$$

Consequently, the nucleon-DM effective interaction can be written as

$$\mathcal{L}_{\text{DM}-\mathcal{N}}^{(eff)} = a_{\mathcal{N}} \bar{\mathcal{N}} \mathcal{N} N_{\text{DM}}^c N_{\text{DM}}, \quad (42)$$

with

$$a_{\mathcal{N}} = \frac{s_h c_h (M_{\mathcal{N}} - \frac{7}{9} M_{\mathcal{B}}) M_{\text{DM}}}{v x} \left[ \frac{1}{M_{h_1}^2} - \frac{1}{M_{h_2}^2} \right]. \quad (43)$$

In this relation,  $M_{\mathcal{N}}$  is the nucleon mass and  $M_{\mathcal{B}}$  the baryon mass in the chiral limit [28]. Thus, the approximate expression of the spin-independent nucleon-DM elastic cross section at low momentum transfer reads

$$\sigma_{\text{det}} = \frac{s_h^2 c_h^2 M_{\mathcal{N}}^2 (M_{\mathcal{N}} - \frac{7}{9} M_{\mathcal{B}})^2 M_{\text{DM}}^4}{\pi v^2 x^2 (M_{\text{DM}} + M_{\mathcal{B}})^2} \left[ \frac{1}{M_{h_1}^2} - \frac{1}{M_{h_2}^2} \right]^2. \quad (44)$$

As will be discussed below, the most stringent constraint on  $\sigma_{\text{det}}$  comes from the present upped bound reported by LUX experiment [29].

## 6 Numerical Analysis and Results

In our numerical scan we enforce the minimization conditions, Eqs. (6) and (7), vacuum stability, the Higgs mass  $M_{h_2} = 125.09 \pm 0.21$  GeV, as well as the constraints from LEP (OPAL) on a light Higgs [30]. The constraint from the Higgs invisible decay  $\mathcal{B}(h \rightarrow \text{inv}) < 17\%$  [23] is also enforced. All dimensionless couplings are restricted to perturbative values and we consider the range  $200 \text{ GeV} < \langle \phi \rangle < 5 \text{ TeV}$  for the beyond-SM VEV. We find a range of viable values for  $M_{h_2}$ , consistent with the OPAL bounds, as shown in Figure 2. For the parameter space in our scan we tend to find  $M_{h_2}$  in the range  $\mathcal{O}(1) \text{ GeV} \lesssim M_{h_2} \lesssim \mathcal{O}(120) \text{ GeV}$ . Lighter values of  $M_{h_2}$  appear to require a degree of engineered cancellation among the radiative mass-corrections from fermions and bosons; see Eq. (16). We noticed that regions with  $\langle \phi \rangle \gtrsim 700 \text{ GeV}$  tend to be preferred in our scans.

We also scan for viable neutrino masses and mixing, subject to the LFV and muon anomalous magnetic moment constraints, while also demanding a viable DM relic density. In Figure 3 we plot viable benchmark points for the Yukawa couplings  $g_{i\alpha}$  and  $f_{\alpha\beta}$ , along with the corresponding LFV branching ratios and  $\delta a_\mu$  contributions. It is clear that the couplings  $f_{\alpha\beta}$  are generally smaller than the couplings  $g_{i\alpha}$ , and that the bound on  $\tau \rightarrow \mu \gamma$  is readily satisfied, while the constraint from  $\mu \rightarrow e \gamma$  is more severe. We note that, when considering only one or two generations of singlet fermions, no solutions that simultaneously accommodate the neutrino mass and mixing data, low-energy flavor constraints, and the DM relic density, were found. Therefore at least three generations of exotic fermions are required. Also, we verified that the constraints from neutrino-less double-beta decay searches are easily satisfied for all benchmark points.

Recall that, with regards to the DM relic density, there are two classes of annihilation channels, namely  $N_{\text{DM}} N_{\text{DM}} \rightarrow l_\alpha^- l_\beta^+$  and  $N_{\text{DM}} N_{\text{DM}} \rightarrow hh$ . ( $h \equiv h_{1,2}$ ). For heavy DM ( $M_{\text{DM}} > M_{h_2}$ ) both annihilation channels can be available, while for lighter DM the scalar channels are kinematically forbidden. In order to probe the role of each channel, we plot the cross section ratio  $\sigma_{hh}/\sigma_{l_\alpha^- l_\beta^+}$  at the freeze-out versus the DM mass in Figure 4-left. We see that the channel  $N_{\text{DM}} N_{\text{DM}} \rightarrow l_\alpha^- l_\beta^+$  is always dominant except for few benchmark points with the dark matter mass in the range  $25 \text{ GeV} < M_{\text{DM}} < 200 \text{ GeV}$ , while the channel  $N_{\text{DM}} N_{\text{DM}} \rightarrow hh$  is only significant for some benchmarks with  $40 \text{ GeV} < M_{\text{DM}} < 700 \text{ GeV}$ . Figure 4-right shows

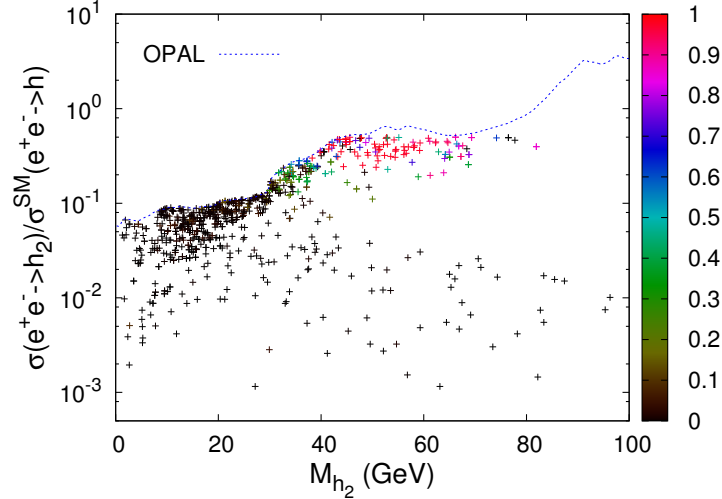


Figure 2: Scalar mixing versus the light scalar mass. The palette gives the branching ratio for invisible Higgs decays, with an overwhelming majority of the points shown satisfying the constraint  $B(h_1 \rightarrow inv) < 17\%$ .

the corresponding charged scalar masses. For lighter DM masses of  $M_{\text{DM}} < 300$  GeV, the charged scalar masses  $M_{S_{1,2}}$  should not exceed 400 GeV, while for larger values of  $M_{\text{DM}}$ , the scalar masses  $M_{S_{1,2}}$  can be at the TeV scale. Such light charged scalars can be within reach of collider experiments [31].

Next we discuss the constraints from direct-detection experiments. We plot the direct-detection cross section versus the DM mass for our benchmark points in Figure 5. One observes immediately that the direct-detection limits impose serious constraints on the model, with a large number of the benchmarks excluded by LUX [29]. We find that only few benchmarks with  $M_{\text{DM}} \lesssim 10$  GeV or  $M_{\text{DM}} \gtrsim 400$  GeV survive the LUX bounds. As is clear from the figure, the surviving benchmarks will be subject to future tests in forthcoming direct-detection experiments. The palette in Figure 5 shows the corresponding values for  $M_{h_2}$ , in units of GeV. In the region of parameter space for which  $N_{\text{DM}}$  is a viable dark matter, we find that the light scalar has to be either lighter than 20 GeV or heavier than 400 GeV. Benchmarks with intermediate values of  $M_{\text{DM}}$  tend to be excluded by the LUX constraints.

We emphasize that we only found a few benchmarks for which the DM relic density was primarily determined by annihilations into scalars. On the surface, this claim may appear contrary to the results of Refs. [32, 33], which consider Majorana DM coupled to a singlet scalar that communicates with the SM via the Higgs portal (called the Indirect Higgs Portal [32]). Naively one may expect our model to admit parameter space where the DM relic-density is determined primarily by the annihilations  $N_{\text{DM}} N_{\text{DM}} \rightarrow hh$ , in analogy with the results of Refs. [32, 33]. However, due to the SI symmetry, our model contains no bare mass terms, which reduces the number of free parameters in the Lagrangian. Consequently the DM mass  $M_{\text{DM}}$  is related to both the coupling between  $N_{\text{DM}}$  and  $\phi$ , and the mixing angle  $\theta_h$ . This reduction in parameters means we cannot evade the LUX constraints whilst generating a viable relic density by annihilations into scalars. This explains the difference between our results and Refs. [32, 33]. It also explains some features of the benchmark distributions in Figure 4-left and Figure 5. The benchmarks in Figure 4-left with large contributions from the channel

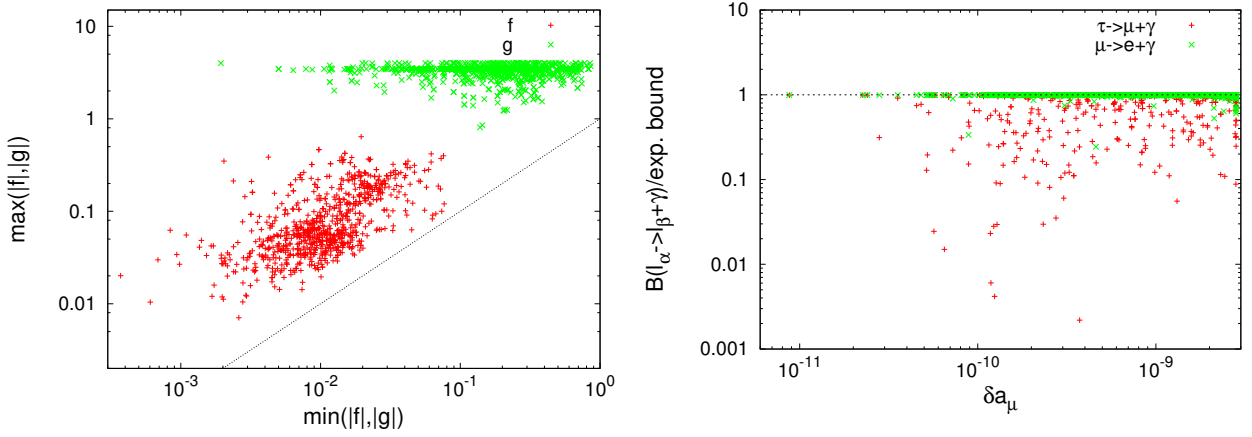


Figure 3: Left: Viable benchmark points for the Yukawa couplings  $g_{i\alpha}$  and  $f_{\alpha\beta}$ , in absolute values, where the dashed line represents the fully degenerate case, i.e,  $\min |f| = \max |f|$ . Right: The LFV branching ratios, scaled by the experimental bounds, versus the muon anomalous magnetic moment.

$N_{\text{DM}} N_{\text{DM}} \rightarrow hh$  have a stronger coupling between  $N_{\text{DM}}$  and  $\phi$ . This stronger coupling increases the direct-detection cross section due to  $h_{1,2}$  exchange, creating conflict with the bounds from LUX. The corresponding benchmarks are strongly ruled out, as seen in Figure 5. Indeed, with the smaller number of parameters in the SI model, it is a non-trivial result that viable regions of parameter space were found in Figure 5.

Finally, we mention that the exotics in the model allow for new contributions to the Higgs decays  $h \rightarrow \gamma\gamma$  and  $h \rightarrow \gamma Z$ . We plot the ratio of the corresponding widths relative to the SM values in Figure 6-right. We observe that most of the benchmarks are consistent with existing constraints from ATLAS and CMS. Importantly, the model can be probed through more precise measurements by ATLAS and CMS after Run II. We note that all benchmark points are consistent with the oblique parameter constraints, as shown in Figure 6-left.

## 7 Conclusion

We presented a scale-invariant extension of the SM in which both the weak scale and neutrino mass were generated radiatively. The model contains a DM candidate, in the form of a sterile neutrino  $N_{\text{DM}}$ . A new light neutral scalar is also predicted, namely the pseudo Goldstone-boson associated with the broken scale-invariance,  $h_2$ , along with two charged scalars  $S_{1,2}$ . The masses for the latter are generically expected to be near the TeV scale, due to the related birth of the exotic scale and the weak scale via dimensional transmutation. The constraints on the model are rather strong, particularly the direct-detections constraints from LUX. However, we demonstrated the existence of viable parameter space with  $M_{\text{DM}} \lesssim 10$  GeV or  $M_{\text{DM}} \gtrsim 400$  GeV. The model can be tested in a number of ways, including future direct-detection experiments, collider searches for the charged scalars, improved LFV searches, and precision measurements of the Higgs decay width to neutral gauge bosons. In a partner paper we shall study the scale-invariant implementation of the Ma model in Ref. [4].

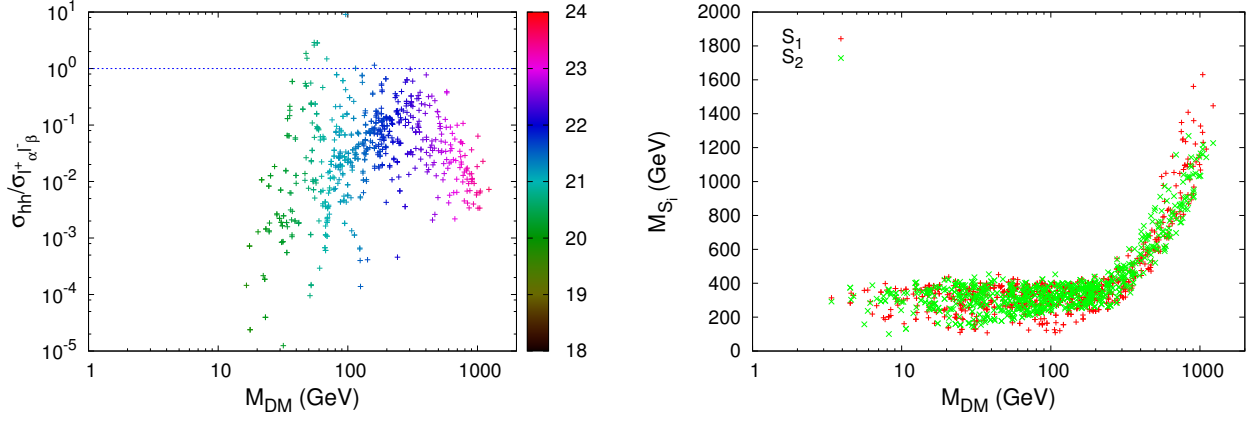


Figure 4: Left: The cross section ratio  $\sigma_{hh}/\sigma_{l_\alpha^- l_\beta^+}$  at the freeze-out temperature versus the DM mass. The palette shows the freeze-out parameter  $x_f = M_{DM}/T_f$  where  $T_f$  is the temperature at which the DM decouples from the thermal bath. Right: The corresponding charged scalar masses versus the DM mass.

## Acknowledgments

AA wants to thank the ICTP for the hospitality during the last stage of this work. AA is supported by the Algerian Ministry of Higher Education and Scientific Research under the CNEPRU Project No D01720130042. KM is supported by the Australian Research Council.

## A Oblique Parameter Functions

The functions employed in the calculation of the oblique parameters in Section 4 are defined as follows:

$$F(I, J) \equiv \begin{cases} \frac{I+J}{2} - \frac{IJ}{I-J} \ln \frac{I}{J} & \Leftarrow I \neq J, \\ 0 & \Leftarrow I = J, \end{cases} \quad (45)$$

$$G(I, J, Q) \equiv -\frac{16}{3} + \frac{5(I+J)}{Q} - \frac{2(I-J)^2}{Q^2} + \frac{3}{Q} \left[ \frac{I^2 + J^2}{I-J} - \frac{I^2 - J^2}{Q} + \frac{(I-J)^3}{3Q^2} \right] \ln \frac{I}{J} + \frac{r}{Q^3} f(t, r), \quad (46)$$

$$\hat{G}(I, Q) = -\frac{79}{3} + 9\frac{I}{Q} - 2\frac{I^2}{Q^2} + \left( -10 + 18\frac{I}{Q} - 6\frac{I^2}{Q^2} + \frac{I^3}{Q^3} - 9\frac{I+Q}{I-Q} \right) \ln \frac{I}{Q} + \left( 12 - 4\frac{I}{Q} + \frac{I^2}{Q^2} \right) \frac{f(I, I^2 - 4IQ)}{Q}, \quad (47)$$

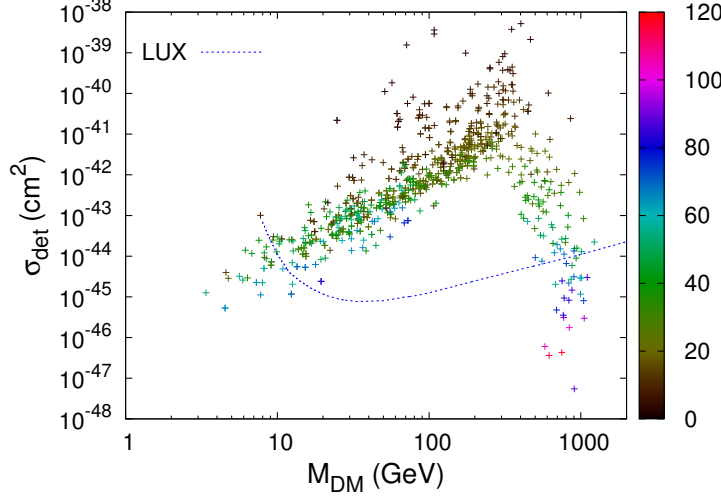


Figure 5: The direct detection cross section versus the DM mass compared to the recent results from LUX. The palette shows the mass for the neutral beyond-SM scalar,  $M_{h_2}$ , in units of GeV.

with  $t \equiv I + J - Q$  and  $r \equiv Q^2 - 2Q(I + J) + (I - J)^2$ , and

$$f(t, r) \equiv \begin{cases} \sqrt{r} \ln \left| \frac{t - \sqrt{r}}{t + \sqrt{r}} \right| & \Leftarrow r > 0, \\ 0 & \Leftarrow r = 0, \\ 2\sqrt{-r} \arctan \frac{\sqrt{-r}}{t} & \Leftarrow r < 0. \end{cases} \quad (48)$$

## B Loop induced Higgs decay functions

The functions used to evaluate the Higgs decay rate of  $h \rightarrow \gamma\gamma$  are given by

$$\begin{aligned} A_0^{\gamma\gamma}(x) &= -x^{-2} [x - f(x)], \\ A_{1/2}^{\gamma\gamma}(x) &= 2x^{-2} [x + (x - 1)f(x)], \\ A_1^{\gamma\gamma}(x) &= -x^{-2} [2x^2 + 3x + 3(2x - 1)f(x)], \end{aligned} \quad (49)$$

with

$$f(x) = \begin{cases} \arcsin^2(\sqrt{x}) & x \leq 1 \\ -\frac{1}{4} \left[ \log \frac{1 + \sqrt{1 - x^{-1}}}{1 - \sqrt{1 - x^{-1}}} - i\pi \right]^2 & x > 1, \end{cases} \quad (50)$$

and those used in the decay rate of  $h \rightarrow \gamma Z$  are given by

$$\begin{aligned} A_0^{\gamma Z}(x, y) &= I_1(x, y), \\ A_{1/2}^{\gamma Z}(x, y) &= I_1(x, y) - I_2(x, y), \\ A_1^{\gamma Z}(x, y) &= [(1 + 2x)\tan^2 \theta_w - (5 + 2x)] I_1(x, y) + 4(3 - \tan^2 \theta_w) I_2(x, y), \end{aligned} \quad (51)$$



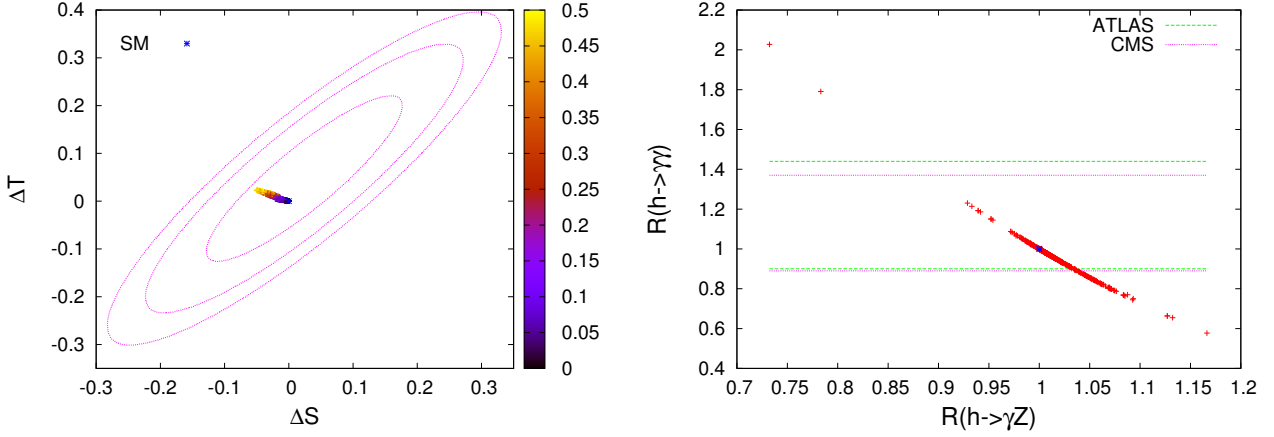


Figure 6: Left: The oblique parameters  $\Delta S$  versus  $\Delta T$  for the benchmarks used previously. The palette shows the mixing  $\sin^2 \theta_h$  and all the points are inside the ellipsoid of 68% CL. Right: Ratio of the widths for  $h \rightarrow \gamma\gamma$  and  $h \rightarrow \gamma Z$  relative to the SM values. The constraints from ATLAS and CMS are shown, along with projected sensitivities after Run II at the LHC.

with

$$I_1(x, y) = -\frac{1}{2(x-y)} + \frac{f(x)-f(y)}{2(x-y)^2} + \frac{y[g(x)-g(y)]}{(x-y)^2}, \quad I_2(x, y) = \frac{f(x)-f(y)}{2(x-y)}, \quad (52)$$

and

$$g(x) = \begin{cases} \sqrt{x^{-1}-1} \arcsin(\sqrt{x}) & x \leq 1 \\ \frac{\sqrt{1-x^{-1}}}{2} \left[ \log \frac{1+\sqrt{1-x^{-1}}}{1-\sqrt{1-x^{-1}}} - i\pi \right] & x > 1. \end{cases} \quad (53)$$

## References

- [1] S. R. Coleman and E. J. Weinberg, Phys. Rev. D **7**, 1888 (1973).
- [2] A. Kobakhidze and K. L. McDonald, JHEP **1407**, 155 (2014) [arXiv:1404.5823 [hep-ph]].
- [3] L. M. Krauss, S. Nasri and M. Trodden, Phys. Rev. D **67**, 085002 (2003) [hep-ph/0210389].
- [4] E. Ma, Phys. Rev. D **73**, 077301 (2006) [hep-ph/0601225]; Phys. Rev. Lett. **102**, 051805 (2009) [arXiv:0807.0361 [hep-ph]]; Phys. Rev. D **80**, 033007 (2009) [arXiv:0904.3829 [hep-ph]]; M. Aoki, S. Kanemura, T. Shindou and K. Yagyu, JHEP **1007**, 084 (2010) [JHEP **1011**, 049 (2010)] [arXiv:1005.5159 [hep-ph]]; S. Kanemura, O. Seto and T. Shimomura, Phys. Rev. D **84**, 016004 (2011) [arXiv:1101.5713 [hep-ph]]; M. Aoki, S. Kanemura and K. Yagyu, Phys. Lett. B **702**, 355 (2011) [Erratum-ibid. B **706**, 495 (2012)] [arXiv:1105.2075 [hep-ph]]; M. Lindner, D. Schmidt and T. Schwetz, Phys. Lett. B **705**, 324 (2011) [arXiv:1105.4626 [hep-ph]]; Phys. Rev. D **85**, 033004 (2012) [arXiv:1111.0599 [hep-ph]]; Y. H. Ahn and H. Okada, Phys. Rev. D **85**, 073010 (2012) [arXiv:1201.4436 [hep-ph]]; S. S. C. Law and K. L. McDonald, Phys. Lett. B **713**, 490 (2012) [arXiv:1204.2529 [hep-ph]]; G. Guo, X. -G. He and G. -N. Li, JHEP **1210**, 044

- (2012) [arXiv:1207.6308 [hep-ph]]; Phys. Rev. D **87**, 053007 (2013) [arXiv:1212.3808 [hep-ph]]; M. Gustafsson, J. M. No and M. A. Rivera, Phys. Rev. Lett. **110**, no. 21, 211802 (2013) [arXiv:1212.4806 [hep-ph]].
- [5] A. Ahriche and S. Nasri, JCAP **1307**, 035 (2013) [arXiv:1304.2055]; A. Ahriche, C. S. Chen, K. L. McDonald and S. Nasri, Phys. Rev. D **90**, 015024 (2014) [arXiv:1404.2696 [hep-ph]]; A. Ahriche, K. L. McDonald and S. Nasri, JHEP **1410**, 167 (2014) [arXiv:1404.5917 [hep-ph]]; C. S. Chen, K. L. McDonald and S. Nasri, Phys. Lett. B **734**, 388 (2014) [arXiv:1404.6033 [hep-ph]]; A. Ahriche, K. L. McDonald, S. Nasri and T. Toma, arXiv:1504.05755 [hep-ph].
- [6] M. Aoki, J. Kubo and H. Takano, Phys. Rev. D **87**, 116001 (2013) [arXiv:1302.3936 [hep-ph]]. Nucl. Phys. B **874**, 198 (2013) [arXiv:1303.3463 [hep-ph]]; Y. Kajiyama, H. Okada and T. Toma, Phys. Rev. D **88**, no. 1, 015029 (2013) [arXiv:1303.7356]; S. S. C. Law and K. L. McDonald, JHEP **1309**, 092 (2013) [arXiv:1305.6467 [hep-ph]]; D. Restrepo, O. Zapata and C. E. Yaguna, JHEP **1311**, 011 (2013) [arXiv:1308.3655 [hep-ph]]; E. Ma, I. Picek and B. Radovic Phys. Lett. B **726**, 744 (2013) [arXiv:1308.5313 [hep-ph]]; V. Brdar, I. Picek and B. Radovic, Phys. Lett. B **728**, 198 (2014) [arXiv:1310.3183 [hep-ph]]; H. Okada and K. Yagyu, Phys. Rev. D **89**, no. 5, 053008 (2014) [arXiv:1311.4360 [hep-ph]]; S. Baek, H. Okada and T. Toma, arXiv:1312.3761 [hep-ph]; S. Baek, H. Okada and T. Toma, arXiv:1401.6921 [hep-ph]; H. Okada, arXiv:1404.0280 [hep-ph]; S. Nasri, Phys. Rev. D **90**, 015024 (2014) [arXiv:1404.2696 [hep-ph]].
- [7] J. N. Ng and A. de la Puente, Phys. Rev. D **90**, no. 9, 095018 (2014) [arXiv:1404.1415 [hep-ph]]; S. Kanemura, T. Matsui and H. Sugiyama, Phys. Rev. D **90**, 013001 (2014) [arXiv:1405.1935 [hep-ph]]; H. Okada and K. Yagyu, Phys. Rev. D **90**, 035019 (2014) [arXiv:1405.2368 [hep-ph]]; S. Kanemura, N. Machida and T. Shindou, Phys. Lett. B **738**, 178 (2014) [arXiv:1405.5834 [hep-ph]]; M. Aoki and T. Toma, JCAP **1409**, 016 (2014) [arXiv:1405.5870 [hep-ph]]; H. Ishida and H. Okada, arXiv:1406.5808 [hep-ph]; H. Okada and Y. Orikasa, Phys. Rev. D **90**, 075023 (2014) [arXiv:1407.2543 [hep-ph]]; H. Okada, T. Toma and K. Yagyu, Phys. Rev. D **90**, 095005 (2014) [arXiv:1408.0961 [hep-ph]]; H. Hatanaka, K. Nishiwaki, H. Okada and Y. Orikasa, arXiv:1412.8664 [hep-ph]; S. Baek, H. Okada and K. Yagyu, arXiv:1501.01530 [hep-ph]; L. G. Jin, R. Tang and F. Zhang, Phys. Lett. B **741**, 163 (2015) [arXiv:1501.02020 [hep-ph]]; H. Okada, arXiv:1503.04557 [hep-ph]; H. Okada, N. Okada and Y. Orikasa, arXiv:1504.01204 [hep-ph].
- [8] P. Culjak, K. Kumericki and I. Picek, Phys. Lett. B **744**, 237 (2015) [arXiv:1502.07887 [hep-ph]]; D. Restrepo, A. Rivera, M. Sanchez-Pelaez, O. Zapata and W. Tangarife, arXiv:1504.07892 [hep-ph]; S. Kashiwase, H. Okada, Y. Orikasa and T. Toma, arXiv:1505.04665 [hep-ph]; T. A. Chowdhury and S. Nasri, arXiv:1506.00261 [hep-ph]; M. Aoki, T. Toma and A. Vicente, arXiv:1507.01591 [hep-ph]; K. Nishiwaki, H. Okada and Y. Orikasa, arXiv:1507.02412 [hep-ph]. W. Wang and Z. L. Han, arXiv:1508.00706 [hep-ph].
- [9] R. Hempfling, Phys. Lett. B **379**, 153 (1996) [hep-ph/9604278]; K. A. Meissner and H. Nicolai, Phys. Lett. B **648**, 312 (2007) [hep-th/0612165]; W. F. Chang, J. N. Ng and J. M. S. Wu, Phys. Rev. D **75**, 115016 (2007) [hep-ph/0701254 [HEP-PH]]; R. Foot, A. Kobakhidze and R. R. Volkas, Phys. Lett. B **655**, 156 (2007) [arXiv:0704.1165 [hep-ph]]; R. Foot, A. Kobakhidze, K. L. McDonald and R. R. Volkas, Phys. Rev. D **76**, 075014

- (2007) [arXiv:0706.1829 [hep-ph]]; R. Foot, A. Kobakhidze and R. R. Volkas, Phys. Rev. D **82** 035005 (2010) [arXiv:1006.0131 [hep-ph]];
- [10] S. Iso, N. Okada and Y. Orikasa, Phys. Lett. B **676**, 81 (2009) [arXiv:0902.4050 [hep-ph]]; *ibid.*, Phys. Rev. D **80**, 115007 (2009) [arXiv:0909.0128 [hep-ph]]; M. Holthausen, M. Lindner and M. A. Schmidt, Phys. Rev. D **82**, 055002 (2010) [arXiv:0911.0710 [hep-ph]]; T. Hur and P. Ko, Phys. Rev. Lett. **106**, 141802 (2011) [arXiv:1103.2571 [hep-ph]]; L. Alexander-Nunneley and A. Pilaftsis, JHEP **1009**, 021 (2010) [arXiv:1006.5916 [hep-ph]]; K. Ishiwata, Phys. Lett. B **710**, 134 (2012) [arXiv:1112.2696 [hep-ph]]; J. S. Lee and A. Pilaftsis, Phys. Rev. D **86**, 035004 (2012) [arXiv:1201.4891 [hep-ph]]; N. Okada and Y. Orikasa, Phys. Rev. D **85**, 115006 (2012) [arXiv:1202.1405 [hep-ph]]; S. Iso and Y. Orikasa, PTEP **2013**, 023B08 (2013) [arXiv:1210.2848 [hep-ph]]; C. Englert, J. Jaeckel, V. V. Khoze and M. Spannowsky, JHEP **1304**, 060 (2013) [arXiv:1301.4224 [hep-ph]].
- [11] M. Heikinheimo, A. Racioppi, M. Raidal, C. Spethmann and K. Tuominen, Mod. Phys. Lett. A **29** (2014) 1450077 [arXiv:1304.7006 [hep-ph]]; T. Hambye and A. Strumia, Phys. Rev. D **88**, 055022 (2013) [arXiv:1306.2329 [hep-ph]]; I. Bars, P. Steinhardt and N. Turok, Phys. Rev. D **89**, no. 4, 043515 (2014) [arXiv:1307.1848 [hep-th]]; M. Heikinheimo, A. Racioppi, M. Raidal and C. Spethmann, Phys. Lett. B **726**, 781 (2013) [arXiv:1307.7146]; C. D. Carone and R. Ramos, Phys. Rev. D **88**, 055020 (2013) [arXiv:1307.8428 [hep-ph]]; G. Marques Tavares, M. Schmaltz and W. Skiba, Phys. Rev. D **89**, 015009 (2014) [arXiv:1308.0025 [hep-ph]]; A. Farzinnia, H. J. He and J. Ren, Phys. Lett. B **727**, 141 (2013) [arXiv:1308.0295 [hep-ph]]; Y. Kawamura, PTEP **2013**, no. 11, 113B04 (2013) [arXiv:1308.5069 [hep-ph]]; E. Gabrielli, M. Heikinheimo, K. Kannike, A. Racioppi, M. Raidal and C. Spethmann, Phys. Rev. D **89**, no. 1, 015017 (2014) [arXiv:1309.6632 [hep-ph]]; T. G. Steele, Z. W. Wang, D. Contreras and R. B. Mann, Phys. Rev. Lett. **112**, no. 17, 171602 (2014) [arXiv:1310.1960 [hep-ph]]; M. Hashimoto, S. Iso and Y. Orikasa, Phys. Rev. D **89**, no. 1, 016019 (2014) [arXiv:1310.4304 [hep-ph]].
- [12] S. Abel and A. Mariotti, Phys. Rev. D **89**, no. 12, 125018 (2014) [arXiv:1312.5335 [hep-ph]]; C. T. Hill, Phys. Rev. D **89**, no. 7, 073003 (2014) [arXiv:1401.4185 [hep-ph]]; J. Guo and Z. Kang, arXiv:1401.5609 [hep-ph]; M. Hashimoto, S. Iso and Y. Orikasa, Phys. Rev. D **89**, no. 5, 056010 (2014) [arXiv:1401.5944 [hep-ph]]; S. Benic and B. Radovic, Phys. Lett. B **732**, 91 (2014) [arXiv:1401.8183 [hep-ph]]; A. Salvio and A. Strumia, JHEP **1406**, 080 (2014) [arXiv:1403.4226 [hep-ph]]; J. Kubo, K. S. Lim and M. Lindner, Phys. Rev. Lett. **113**, 091604 (2014) [arXiv:1403.4262 [hep-ph]]; V. V. Khoze, C. McCabe and G. Ro, JHEP **1408**, 026 (2014) [arXiv:1403.4953 [hep-ph], arXiv:1403.4953]; G. C. Dorsch, S. J. Huber and J. M. No, Phys. Rev. Lett. **113**, 121801 (2014) [arXiv:1403.5583 [hep-ph]]; H. Davoudiasl and I. M. Lewis, Phys. Rev. D **90**, no. 3, 033003 (2014) [arXiv:1404.6260 [hep-ph]]; J. Kubo, K. S. Lim and M. Lindner, JHEP **1409**, 016 (2014) [arXiv:1405.1052 [hep-ph]]; M. Lindner, S. Schmidt and J. Smirnov, JHEP **1410**, 177 (2014) [arXiv:1405.6204 [hep-ph]].
- [13] K. Kannike, A. Racioppi and M. Raidal, JHEP **1406**, 154 (2014) [arXiv:1405.3987 [hep-ph]]; V. V. Khoze and G. Ro, JHEP **1410**, 61 (2014) [arXiv:1406.2291 [hep-ph]]; D. F. Litim and F. Sannino, JHEP **1412**, 178 (2014) [arXiv:1406.2337 [hep-th]]; G. M. Pelaggi, Nucl. Phys. B **893**, 443 (2015) [arXiv:1406.4104 [hep-ph]]; O. Antipin, E. Mølgaard and F. Sannino, JHEP **1506**, 030 (2015) [arXiv:1406.6166 [hep-th]]. W. Altmannshofer, W. A. Bardeen, M. Bauer, M. Carena and J. D. Lykken, JHEP **1501**, 032

- (2015) [arXiv:1408.3429 [hep-ph]]; Y. Hamada, H. Kawai, K. y. Oda and S. C. Park, Phys. Rev. D **91**, no. 5, 053008 (2015) [arXiv:1408.4864 [hep-ph]]; T. G. Steele, Z. W. Wang and D. G. C. McKeon, Phys. Rev. D **90**, no. 10, 105012 (2014) [arXiv:1409.3489 [hep-ph]]; O. Antipin, M. Redi and A. Strumia, JHEP **1501**, 157 (2015) [arXiv:1410.1817 [hep-ph]]; K. Allison, C. T. Hill and G. G. Ross, Nucl. Phys. B **891**, 613 (2015) [arXiv:1409.4029 [hep-ph]]; M. B. Einhorn and D. R. T. Jones, JHEP **1503**, 047 (2015) [arXiv:1410.8513 [hep-th]]; Z. Kang, arXiv:1411.2773 [hep-ph]; G. F. Giudice, G. Isidori, A. Salvio and A. Strumia, JHEP **1502**, 137 (2015) [arXiv:1412.2769 [hep-ph]]; H. Okada and Y. Orikasa, arXiv:1412.3616 [hep-ph].
- [14] Y. Hamada, H. Kawai and K. y. Oda, arXiv:1501.04455 [hep-ph]; J. Guo, Z. Kang, P. Ko and Y. Orikasa, arXiv:1502.00508 [hep-ph]; K. Kannike, G. HÿtsiA. Salvio and A. Strumia, arXiv:1502.01334 [astro-ph.CO]; N. G. Nielsen, F. Sannino and O. Svendsen, arXiv:1503.00702 [hep-ph]; K. Endo and Y. Sumino, arXiv:1503.02819 [hep-ph]; P. Humbert, M. Lindner and J. Smirnov, arXiv:1503.03066 [hep-ph]; S. Oda, N. Okada and D. s. Takahashi, arXiv:1504.06291 [hep-ph]; Y. Ametani, M. Aoki, H. Goto and J. Kubo, arXiv:1505.00128 [hep-ph]; Y. Hamada, K. Kawana and K. Tsumura, arXiv:1505.01721 [hep-ph]; C. D. Carone and R. Ramos, arXiv:1505.04448 [hep-ph]; Z. Kang, arXiv:1505.06554 [hep-ph]; S. Di Chiara and K. Tuominen, arXiv:1506.03285 [hep-ph]; Y. Hamada and K. Kawana, arXiv:1506.06553 [hep-ph]; J. Kubo and M. Yamada, arXiv:1506.06460 [hep-ph]; K. Endo and K. Ishiwata, arXiv:1507.01739 [hep-ph]; A. Farzinnia, arXiv:1507.06926 [hep-ph]; D. M. Ghilencea, arXiv:1508.00595 [hep-ph].
- [15] R. Foot, A. Kobakhidze, K. L. McDonald and R. R. Volkas, Phys. Rev. D **77**, 035006 (2008) [arXiv:0709.2750 [hep-ph]].
- [16] E. Gildener and S. Weinberg, Phys. Rev. D **13**, 3333 (1976).
- [17] R. Foot, A. Kobakhidze, K. L. McDonald and R. R. Volkas, Phys. Rev. D **89**, 115018 (2014) [arXiv:1310.0223 [hep-ph]].
- [18] B. Pontecorvo, Sov. Phys. JETP **26**, 984 (1968) [Zh. Eksp. Teor. Fiz. **53**, 1717 (1967)]; Z. Maki, M. Nakagawa and S. Sakata, Prog. Theor. Phys. **28**, 870 (1962).
- [19] D. V. Forero, M. Tortola and J. W. F. Valle, Phys. Rev. D **86**, 073012 (2012) [arXiv:1205.4018 [hep-ph]].
- [20] F. Simkovic, A. Faessler, H. Muther, V. Rodin and M. Stauf, Phys. Rev. C **79**, 055501 (2009) [arXiv:0902.0331 [nucl-th]].
- [21] B.W. Lynn, M.E. Peskin, and R.G. Stuart, in *Physics at LEP*, J. Ellis and R.D. Peccei eds. (CERN, Geneva, 1986); D.C. Kennedy and B.W. Lynn, *Nucl. Phys. B* **322** (1989) 1; M.E. Peskin and T. Takeuchi, *Phys. Rev. Lett.* **65** (1990) 964; G. Altarelli and R. Barbieri, *Phys. Lett. B* **253** (1991) 161; M.E. Peskin and T. Takeuchi, *Phys. Rev. D* **46** (1992) 381. G. Altarelli, R. Barbieri, and S. Jadach, *Nucl. Phys. B* **369** (1992) 3 [erratum *ibid. B* **376** (1992) 444].
- [22] W. Grimus, L. Lavoura, O. M. Ogreid and P. Osland, Nucl. Phys. B **801**, 81 (2008) [arXiv:0802.4353 [hep-ph]].
- [23] P. Bechtle, S. Heinemeyer, O. St al, T. Stefaniak, and G. Weiglein, JHEP 1411 (2014) 039, [arXiv:1403.1582].

- [24] A. Djouadi, Phys. Rept. 457 (2008) 1.
- [25] G. Jungman, M. Kamionkowski and K. Griest, Phys. Rept. 267 (1996) 195; G. Bertone, D. Hooper and J. Silk, Phys. Rept. 405 (2005) 279; L. Bergstrom, Rept. Prog. Phys. 63 (2000) 793.
- [26] P. A. R. Ade et al. [Planck Collaboration], arXiv:1502.01589 [astro-ph.CO].
- [27] A. Ahriche, A. Arhrib and S. Nasri, JHEP02 (2014) 042.
- [28] X.G. He, T. Li, X.Q. Li, J. Tandean and H.C. Tsai, Phys. Rev. D79 (2009) 023521 (arXiv:0811.0658 [hep-ph]).
- [29] D. S. Akerib *et al.* [LUX Collaboration], arXiv:1310.8214 [astro-ph.CO].
- [30] OPAL Collaboration (G. Abbiendi et al.), Eur. Phys. J. C27 (2003) 311-329.
- [31] A. Ahriche, S. Nasri and R. Soualah, arXiv:1403.5694 [hep-ph].
- [32] L. Lopez-Honorez, T. Schwetz and J. Zupan, Phys. Lett. B **716**, 179 (2012) [arXiv:1203.2064 [hep-ph]].
- [33] M. Dutra, C. A. d. S. Pires and P. S. R. da Silva, arXiv:1504.07222 [hep-ph].